Available online at www.sciencedirect.com
SCIENCE DIRECT
Journal of Power Sources 158 (2006) 148–153
JOURNAL OF POWER SOURCES
www.elsevier.com/locate/jpowsour

Technical update

Combustion synthesis of $Sm_{0.5}Sr_{0.5}CoO_{3-x}$ and $La_{0.6}Sr_{0.4}CoO_{3-x}$ nanopowders for solid oxide fuel cell cathodes

Narottam P. Bansal [a,*], Zhimin Zhong [b]

[a] National Aeronautics and Space Administration, Glenn Research Center, Cleveland, OH 44135, USA
[b] QSS Group Inc., NASA Glenn Research Center Group, Cleveland, OH 44135, USA

Received 10 August 2005; accepted 1 September 2005
Available online 15 November 2005

Abstract

Nanopowders of $Sm_{0.5}Sr_{0.5}CoO_{3-x}$ (SSC) and $La_{0.6}Sr_{0.4}CoO_{3-x}$ (LSC) compositions, which are being investigated as cathode materials for intermediate temperature solid oxide fuel cells (SOFC), were synthesized by a solution–combustion method using metal nitrates and glycine as fuel. Development of crystalline phases in the as-synthesized powders after heat treatments at various temperatures was monitored by X-ray diffraction (XRD). Perovskite phase in LSC formed more readily than in SSC. Single-phase perovskites were obtained after heat treatment of the combustion synthesized LSC and SSC powders at 1000 and 1200 °C, respectively. The as-synthesized powders had an average particle size of ~12 nm as determined from X-ray line broadening analysis using the Scherrer equation. Average grain size of the powders increased with increase in calcination temperature. Morphological analysis of the powders calcined at various temperatures was done by scanning electron microscopy (SEM).

Keywords: Nanopowder; Solid oxide fuel cells; Cathodes; Powder processing

1. Introduction

Solid oxide fuel cells (SOFC) are being considered [1] as the premium power generation devices in the future as they have demonstrated high-energy conversion efficiency, high power density, extremely low pollution, in addition to flexibility in using hydrocarbon fuel. A major obstacle for commercial applications of SOFC still is high cost, both in terms of materials and processing. Intermediate Temperature-Solid Oxide Fuel Cell (IT-SOFC) operated between 500 and 800 °C, which allows utilization of available and inexpensive interconnects and sealing materials, can significantly reduce the cost of SOFC. The IT-SOFC also will have better reliability and portability. To keep up with the performance of traditional SOFC that operates between 900 and 1000 °C, new materials with improved performance have to be used [2,3]. To enhance the oxygen ion conductivity of the electrolyte at the reduced temperature, $La_{1-x}Sr_xGa_{1-y}Mg_yO_z$ (LSGM), scandium stabilized zirconia or lanthanum (gadolinium, samarium) doped ceria can be used to replace the yttrium stabilized zirconia. Similarly, cathode materials with higher performance at the lower temperature such as $Sm_{0.5}Sr_{0.5}CoO_{3-x}$ (SSC), $La_{0.6}Sr_{0.4}CoO_{3-x}$ (LSC), $La_{0.8}Sr_{0.2}Co_{0.2}Fe_{0.8}O_{3-x}$ (LSCF) will be used to substitute $La_{1-y}Sr_yMnO_{3-x}$ (LSM), the performance of which decreases rapidly when the operating temperature is below 800 °C.

The primary objective of this study was to synthesize fine powders of SSC and LSC compositions for applications as SOFC cathodes. A number of approaches such as, solid-state reaction, sol–gel, hydrothermal, spray-drying, freeze-drying, co-precipitation, and solution–combustion have been used for ceramic powders processing. The solution–combustion method is particularly useful in the production of ultrafine ceramic powders of complex oxide compositions in a relatively short time. This approach has been utilized [4–10] for the synthesis of various oxide powders such as ferrites, chromites, manganites, Ni-YSZ cermet, zirconates, doped ceria, hexa-aluminates, pyrochlores, oxide phosphors, spinels, etc. An amino acid such as glycine is commonly used as the fuel in the combustion process. However, urea, citric acid, oxylydihydrazide, and sucrose

* Corresponding author. Tel.: +1 216 433 3855; fax: +1 216 433 5544.
E-mail address: Narottam.P.Bansal@nasa.gov (N.P. Bansal).

0378-7753/$ – see front matter © 2005 Elsevier B.V. All rights reserved.
doi:10.1016/j.jpowsour.2005.09.057

have also been recently utilized [6,10] as complexing agents and fuel in the combustion synthesis.

In the present study, SSC and LSC cathode powders were synthesized using the glycine-nitrate solution–combustion technique [4–6] because of its high-energy efficiency, fast heating rates, short reaction times, and high reaction temperatures. This process is also unique as all the reactants are mixed in solution at the molecular level resulting in homogeneous reaction products and faster reaction rates. Development of crystalline phases in the powders, on heat treatments at various temperatures, was followed by powder X-ray diffraction (XRD). Morphology of the powders was characterized by scanning electron microscopy (SEM).

2. Experimental methods

2.1. Powder synthesis

The starting materials used in the synthesis were metal nitrates $Sm(NO_3)_3{\cdot}6H_2O$ (99.9% purity), $La(NO_3)_3{\cdot}6H_2O$ (99.9% purity), $Sr(NO_3)_2$ (98% purity), $Co(NO_3)_2{\cdot}6H_2O$ (97.7% purity), and glycine (NH_2CH_2COOH, 99.5% purity), all from Alfa Aesar. A flow chart showing the various steps involved in the synthesis of powders by the solution–combustion process is shown in Fig. 1. Metal nitrates are employed both as metal precursors and oxidizing agents. Stoichiometric amounts of the metal nitrates, to yield 10 g of the final SSC or LSC oxide powder, were dissolved in deionized water. A calculated amount of the amino acid glycine (0.7 mol mol^{-1} of NO_3^-) was also dissolved in deionized water. The glycine solution was slowly added to the metal nitrate aqueous solution under constant stirring. Glycine acts as a complexing agent for metal cations of varying sizes as it has a carboxylic group at one end and an amino group at the other end. The complexation process increases the solubility of metal ions and helps to maintain homogeneity by preventing their selective precipitation. The resulting clear and transparent red colored solution was heated on a hot plate until concentrated to about 2 mol l^{-1} on metal nitrate basis. While the solution was still hot, it was added dropwise to a 2 l glass beaker that was preheated between 300 and 400 °C. The water in the solution quickly evaporated, the resulting viscous liquid swelled, auto-ignited and initiated a highly exothermic self-contained combustion process, converting the precursor materials into fine powder of the complex oxides. Glycine acts as a fuel during the combustion reaction, being oxidized by the nitrate ions. Oxygen from air does not play an important role during the combustion process. The overall combustion reactions can be represented as:

$$0.6La(NO_3)_3 + 0.4Sr(NO_3)_2 + Co(NO_3)_2 + 3.2H_2NCH_2COOH + \left(1.8 - \frac{x}{2}\right) O_2 \rightarrow La_{0.6}Sr_{0.4}CoO_{3-x} + 6.4CO_2 + 8H_2O + 3.9N_2 \quad (1)$$

$$0.5Sm(NO_3)_3 + 0.5Sr(NO_3)_2 + Co(NO_3)_2 + 3.2H_2NCH_2COOH + \left(1.95 - \frac{x}{2}\right) O_2 \rightarrow Sm_{0.5}Sr_{0.5}CoO_{3-x} + 6.4CO_2 + 8H_2O + 3.85N_2 \quad (2)$$

indicating the formation of CO_2, N_2, and H_2O as the gaseous products. The evolution of gases during the combustion process helps in the formation of fine ceramic powder by limiting the inter-particle contact. The resulting black powder contained some carbon residue and was further calcined to convert to the desired product. Small portions (~1 g) of this powder were heat treated in air at various temperatures between 700 and 1300 °C for 2 h to study the development of crystalline phases.

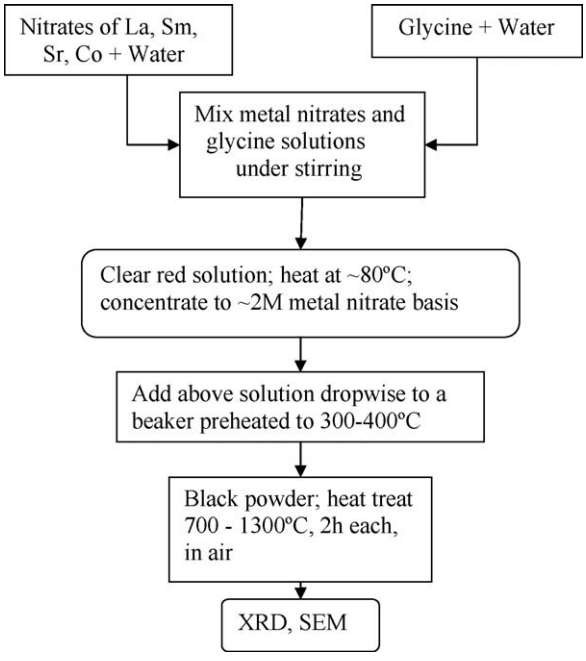

Fig. 1. Flow chart for solution–combustion synthesis of $Sm_{0.5}Sr_{0.5}CoO_{3-x}$ and $La_{0.6}Sr_{0.4}CoO_{3-x}$ nanopowders.

2.2. Characterization

Thermal gravimetric analysis (TGA) of the powders was carried out using a Perkin-Elmer Thermogravimetric Analyzer 7 system which was interfaced with computerized data acquisition and analysis system at a heating rate of 10 °C min^{-1}. Air at 40 ml min^{-1} was used as a purge gas. X-ray diffraction analysis was carried out on powders heat treated at various temperatures for crystalline phase identification and crystallite size determination. Powder XRD patterns were recorded at room temperature using a step scan procedure (0.02°/2θ step, time per step 0.5 or 1 s) in the 2θ range 10–70° on a Philips ADP-3600 automated diffractometer equipped with a crystal monochromator employing Cu Kα radiation. Microstructural analysis was carried out using a JEOL JSM-840A scanning electron microscope. Prior to analysis, a thin layer of Pt or carbon was evaporated onto the SEM specimens for electrical conductivity.

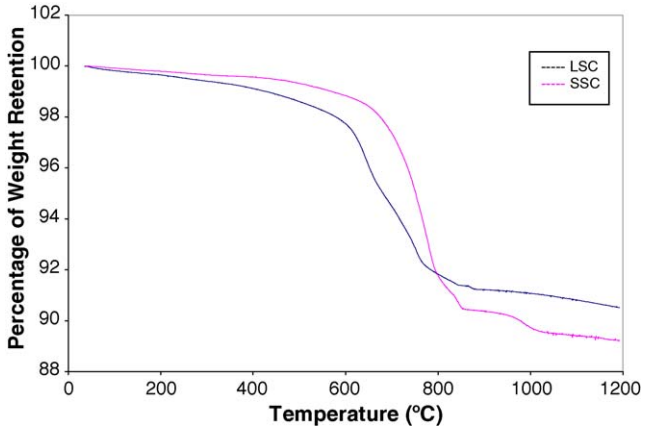

Fig. 2. TGA curves of as-synthesized precursor powders by solution–combustion method for $La_{0.6}Sr_{0.4}CoO_{3-x}$ and $Sm_{0.5}Sr_{0.5}CoO_{3-x}$ at a heating rate of 10 °C min^{-1} in air.

3. Results and discussion

3.1. Thermogravimetric analysis

Fig. 2 shows the TGA curves recorded at a heating rate of 10 °C min^{-1} in air from room temperature to 1200 °C for the as-synthesized LSC and SSC powders using the solution–combustion method. For both precursors, about 6% weight loss was observed between 600 and 850 °C that was likely due to loss of carbon residue by oxidation and also from decomposition of $SrCO_3$. For SSC, there was additional 1% weight loss between 850 and 1000 °C for which there is no simple explanation based on the X-ray diffraction results of Fig. 4.

3.2. Phase formation and microstructure

Both the LSC and SSC as-synthesized powders were calcined in air for 2 h at various temperatures between 700 and 1300 °C to investigate the evolution of crystalline phases. X-ray diffraction patterns for these heat treated LSC and SSC powders are shown in Figs. 3 and 4, respectively and the results are summarized in Table 1. The as-prepared LSC powder shows weak crystallinity of the perovskite phase. $SrCO_3$ phase was also observed in the as-synthesized powder and after calcination at 700 °C. An unknown peak at 32° (probably $Sr_3Co_2O_{6.13}$, 83–375) appeared for the powder calcined at 800 and 900 °C. Formation of the perovskite phase, $La_{0.6}Sr_{0.4}CoO_{3-x}$, is completed above 1000 °C as observed by XRD results in Fig. 3. The as-prepared SSC powder showed the presence of Sm_2O_3, Co_3O_4, and $SrCO_3$ phases. The desired $Sm_{0.5}Sr_{0.5}CoO_{3-x}$ perovskite phase emerged as the major phase after the powder was calcined at 700 °C. Secondary phases such as $Sr_3Co_2O_{6.13}$ remained even after the powder was heat treated at 1100 °C. Perovskite phase-pure $Sm_{0.5}Sr_{0.5}CoO_{3-x}$ powder was obtained on heat treatment at 1200 °C for 2 h. Earlier investigation [7] of synthesis of SSC by solid-state reaction method indicated that the perovskite phase was formed after calcination at 1200 °C for 6 h. The products calcined at this temperature will have low porosity and non-ideal microstructure as cathode materials.

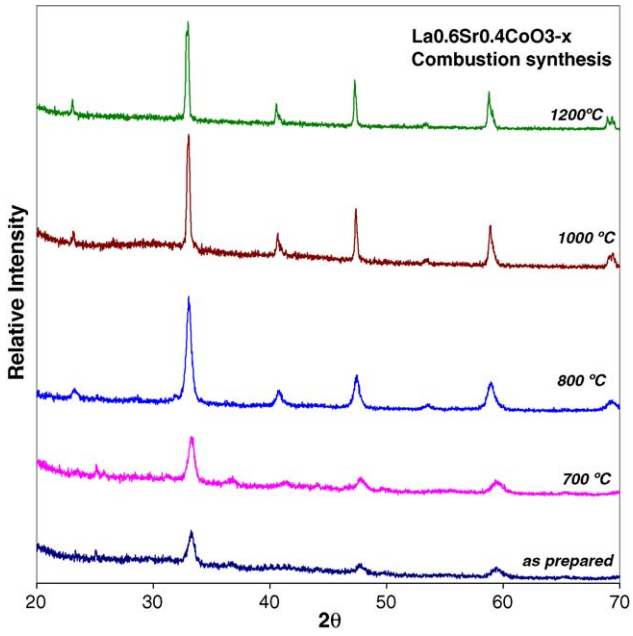

Fig. 3. X-ray diffraction patterns of $La_{0.6}Sr_{0.4}CoO_{3-x}$ powders made by solution–combustion synthesis after heat treatments at various temperatures for 2 h in air.

The SEM micrographs of $La_{0.6}Sr_{0.4}CoO_{3-x}$ and $Sm_{0.5}Sr_{0.5}CoO_{3-x}$ powders made by solution–combustion synthesis after heat treatments at different temperatures for 2 h in

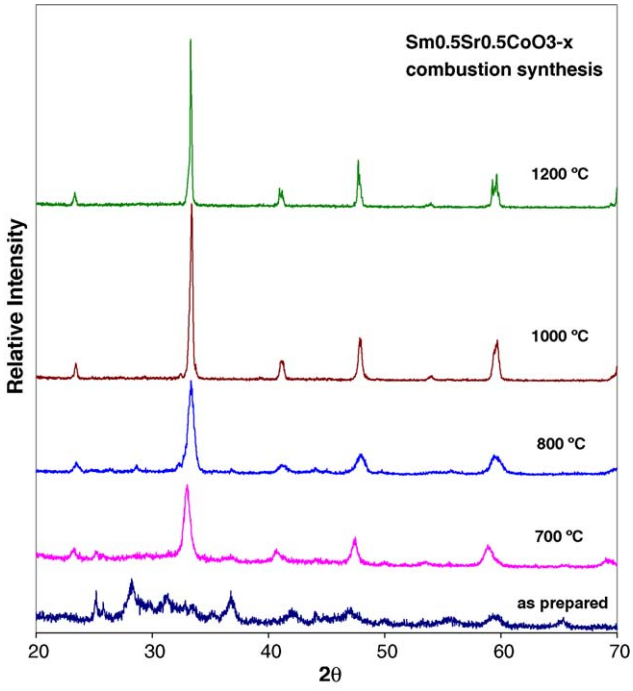

Fig. 4. X-ray diffraction patterns of $Sm_{0.5}Sr_{0.5}CoO_{3-x}$ powders made by solution–combustion synthesis after heat treatments at various temperatures for 2 h in air.

Table 1
X-ray diffraction analysis of $Sm_{0.5}Sr_{0.5}CoO_{3-x}$ and $La_{0.6}Sr_{0.4}CoO_{3-x}$ powders made by solution–combustion synthesis after heat treatments at various temperatures in air

System	Heat treatment		Crystalline phases[a]	Average grain size (nm)[b]
	Temperature (°C)	Time (h)		
$La_{0.6}Sr_{0.4}CoO_{3-x}$	As synthesized	–	$La_{0.6}Sr_{0.4}CoO_{3-x}$, $SrCO_3$	12
	700	2	$La_{0.6}Sr_{0.4}CoO_{3-x}$, $SrCO_3$	15
	800	2	$La_{0.6}Sr_{0.4}CoO_{3-x}$, low intensity peak at 32° 2θ	17
	900	2	$La_{0.6}Sr_{0.4}CoO_{3-x}$, low intensity peak at 32° 2θ	28
	1000	2	$La_{0.6}Sr_{0.4}CoO_{3-x}$	37
	1100	2	$La_{0.6}Sr_{0.4}CoO_{3-x}$	50
	1200	2	$La_{0.6}Sr_{0.4}CoO_{3-x}$	
	1300	2	$La_{0.6}Sr_{0.4}CoO_{3-x}$	
$Sm_{0.5}Sr_{0.5}CoO_{3-x}$	As synthesized	–	Sm_2O_3, Co_3O_4, $SrCO_3$	–
	700	2	$Sm_{0.5}Sr_{0.5}CoO_{3-x}$, $SrCO_3$, Co_3O_4	15
	800	2	$Sm_{0.5}Sr_{0.5}CoO_{3-x}$, $Sr_3Co_2O_{6.13}$, Co_3O_4	15
	900	2	$Sm_{0.5}Sr_{0.5}CoO_{3-x}$, $Sr_3Co_2O_{6.13}$	25
	1000	2	$Sm_{0.5}Sr_{0.5}CoO_{3-x}$, $Sr_3Co_2O_{6.13}$, low intensity peak at 32° 2θ	38
	1100	2	$Sm_{0.5}Sr_{0.5}CoO_{3-x}$, $Sr_3Co_2O_{6.13}$, low intensity peak at 32° 2θ	41
	1200	2	$Sm_{0.5}Sr_{0.5}CoO_{3-x}$	
	1300	2	$Sm_{0.5}Sr_{0.5}CoO_{3-x}$	

[a] Phases in decreasing order of peak intensity.
[b] Calculated from Scherrer formula using FWHM of XRD peak in 47°–48° range of 2θ.

air are presented in Figs. 5 and 6, respectively. The as prepared powders were highly porous and particles were linked together in agglomerates of different shapes and sizes. Substantial particle growth was observed upon calcination for 2 h at 1000 °C or higher temperatures. The particle size of samples calcined at 1000 °C increased but the structure remained highly porous, which resembled the typical cathode structure for SOFC. Therefore, LSC and SSC powders should be sintered around 1000 °C for fabrication of cathode structures. After calcination at 1200 °C, LSC became dense and lost porosity. SSC powder sintered into a dense pellet following heat treatment at 1200 °C.

3.3. Particle size analysis

After each heat treatment of the as-synthesized LSC and SSC powders, the average particle size was evaluated from X-ray line broadening analysis using the Scherrer equation [11]:

$$t = \frac{0.9\lambda}{B\cos\theta_B} \tag{3}$$

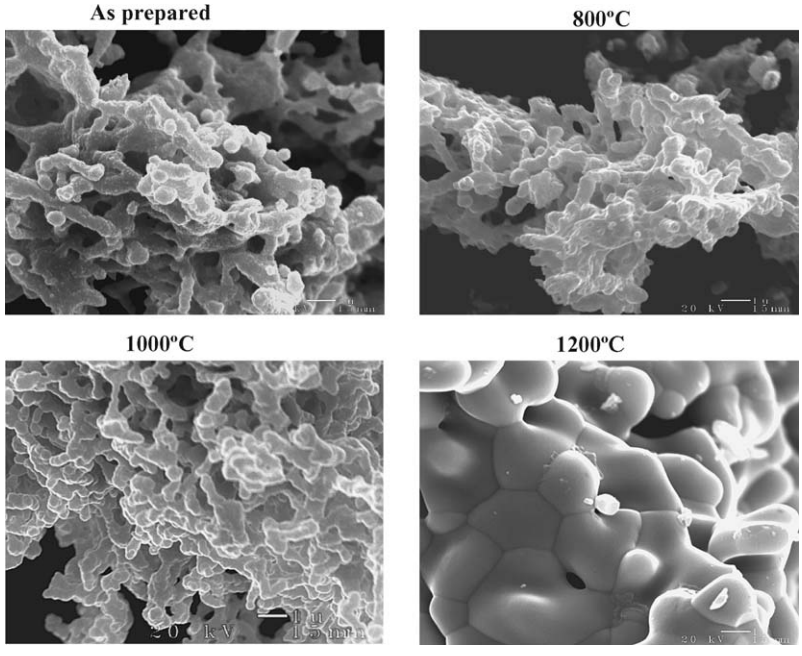

Fig. 5. SEM micrographs of $La_{0.6}Sr_{0.4}CoO_{3-x}$ powders made by solution–combustion synthesis after heat treatments at different temperatures for 2 h in air.

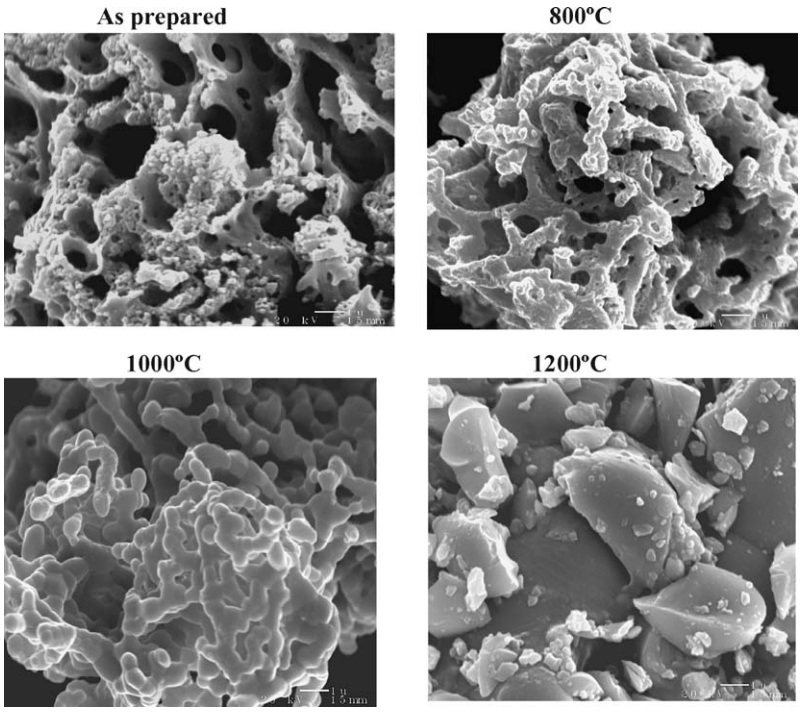

Fig. 6. SEM micrographs of $Sm_{0.5}Sr_{0.5}CoO_{3-x}$ powders made by solution–combustion synthesis after heat treatments at different temperatures for 2 h in air.

where t is the average particle size, λ the wave length of Cu Kα radiation, B the width (in radian) of the XRD diffraction peak at half its maximum intensity, and θ_B the Bragg diffraction angle of the line. Correction for the line broadening by the instrument was applied using a large particle size silicon standard and the relationship

$$B^2 = B_M^2 - B_S^2 \quad (4)$$

where B_M and B_S are the measured widths, at half maximum intensity, of the lines from the sample and the standard, respectively. Values of average grain sizes of the as-synthesized SSC and LSC powders and of those after heat treatments at various temperatures are given in Table 1. The as-synthesized powders had an average grain size of about 10–12 nm. A number of factors are responsible for the nanosize of the resulting powders. Before the reaction, all the reactants are uniformly mixed in solution at atomic or molecular level. So, during combustion, the nucleation process can occur through the rearrangement and short-distance diffusion of nearby atoms and molecules. Also, large volume of the gases evolved during the combustion reactions (1) and (2) limit the inter-particle contact. Moreover, the combustion process occurs at such a fast rate that sufficient energy and time are not available for long-distance diffusion or migration of the atoms or molecules which would result in growth of crystallites. Consequently, the initial nanosize of the powders is retained after the combustion reaction.

The X-ray line broadening method can be used only for the size determination of small crystallites (~100 nm). The values obtained are not the true particle size, but the average size of coherently diffracting domains; the latter being usually much smaller than the actual size of the particles. The crystallite size of the as-synthesized powder depends [8,9] on the glycine to nitrate ratio used during the combustion synthesis. Powder made using a fuel-deficient system has the highest surface area. The powder surface area decreases as the glycine to nitrate ratio is increased. This has been attributed to an increase in the flame temperature during combustion which helps in the growth of crystal size. The average grain size of the SSC and LSC powders increased (Table 1) with the increase in calcination temperature, as expected.

4. Summary and conclusions

Nanopowders of $Sm_{0.5}Sr_{0.5}CoO_{3-x}$ and $La_{0.6}Sr_{0.4}CoO_{3-x}$ cathode materials for solid oxide fuel cells have been synthesized by the glycine-nitrate solution–combustion method. Formation of crystalline phases in both the powders started at relatively low temperatures. However, the as-synthesized powders had to be calcined at or above 1000 °C to yield phase-pure perovskite products. The high temperature calcination caused significant reduction in surface area, coarsening of the powders, and sintering which is not favorable for forming the cathode structures for SOFC. The investigations of electrochemical activity of these materials and co-sintering with fuel cell electrolytes are being investigated and will be presented in the future.

Acknowledgments

Thanks are due to Ralph Garlick for X-ray diffraction analysis. This work was supported by Low Emissions Alternative

Power (LEAP) Project of the Vehicle Systems Program at NASA Glenn Research Center.

References

[1] N.Q. Minh, Ceramic fuel cells, J. Am. Ceram. Soc. 76 (3) (1993) 563–588.
[2] D. Stover, H.P. Buchkremer, S. Uhlenbruck, Processing and properties of the ceramic conductive multilayer device SOFC, Ceram. Int. 30 (7) (2004) 1107–1113.
[3] Y. Liu, S. Zha, M. Liu, Adv. Mater. 16 (3) (2004) 256–260.
[4] S.-J. Kim, W. Lee, W.-J. Lee, S.D. Park, J.S. Song, E.G. Lee, Preparation of nanocrystalline nickel oxide-yttria-stabilized zirconia composite powder by solution combustion with ignition of glycine fuel, J. Mater. Res. 16 (12) (2001) 3621–3627.
[5] L.A. Chick, L.R. Pederson, G.D. Maupin, J.L. Bates, L.E. Thomas, G.J. Exarhos, Glycine-nitrate combustion synthesis of oxide ceramic powders, Mater. Lett. 10 (1990) 6–12.
[6] M. Marinsek, K. Zupan, J. Maeek, Ni-YSZ cermet anodes prepared by citrate/nitrate combustion synthesis, J. Power Sources 106 (2002) 178–188.
[7] T. Ishihara, M. Honda, T. Shibayama, H. Minami, H. Nishiguchi, Y. Takita, Intermediate temperature SOFCs using a new $LaGaO_3$ based oxide ion conductor. I. doped $SmCoO_3$ as a new cathode material, J. Electrochem. Soc. 145 (9) (1998) 3177–3183.
[8] R.D. Purohit, S. Saha, A.K. Tyagi, Nanocrystalline thoria powders via glycine-nitrate combustion, J. Nucl. Mater. 288 (1) (2001) 7–10.
[9] T. Ye, Z. Guiwen, Z. Weiping, X. Shangda, Combustion synthesis and photoluminescence of nanocrystalline Y_2O_3: Eu phosphors, Mater. Res. Bull. 32 (1997) 501.
[10] K. Prabhakaran, J. Joseph, N.M. Gokhale, S.C. Sharma, R. Lal, Sucrose combustion synthesis of $La_xSr_{(1-x)}MnO_3$ ($x \leq 0.2$) powders, Ceram. Int. 31 (2) (2005) 327–331.
[11] B.D. Cullity, Elements of X-Ray Diffraction, second ed., Addison-Wesley, Reading, MA, 1978, p. 284.